Mechanical properties of graphene and boronitrene

R. C. Andrew,[1,*] R. E. Mapasha,[1] A. M. Ukpong,[1] and N. Chetty[1,2]
[1]*Physics Department, University of Pretoria, Pretoria 0002, South Africa*
[2]*National Institute for Theoretical Physics, Johannesburg 2000, South Africa*

We present an equation of state (EOS) that describes how the hydrostatic change in surface area is related to two-dimensional in-plane pressure ($\mathcal{F}$) and yields the measure of a material's resilience to isotropic stretching (the layer modulus γ) as one of its fit parameters. We give results for the monolayer systems of graphene and boronitrene, and we also include results for Si, Ge, GeC, and SiC in the isostructural honeycomb structure for comparison. Our results show that, of the honeycomb structures, graphene is the most resilient to stretching with a value of $\gamma_{\mathrm{C}} = 206.6$ N m^{-1}, second is boronitrene with $\gamma_{\mathrm{BN}} = 177.0$ N m^{-1}, followed by $\gamma_{\mathrm{SiC}} = 116.5$ N m^{-1}, $\gamma_{\mathrm{GeC}} = 101.0$ N m^{-1}, $\gamma_{\mathrm{Si}} = 44.5$ N m^{-1}, and $\gamma_{\mathrm{Ge}} = 29.6$ N m^{-1}. We calculate the Young's and shear moduli from the elastic constants and find that, in general, they rank according to the layer modulus. We also find that the calculated layer modulus matches the one obtained from the EOS. We use the EOS to predict the isotropic intrinsic strength of the various systems and find that, in general, the intrinsic stresses also rank according to the layer modulus. Graphene and boronitrene have comparable strengths with intrinsic stresses of 29.4 and 26.0 N m^{-1}, respectively. We considered four graphene allotropes including pentaheptite and graphdiyne and find that pentaheptite has a value for γ comparable to graphene. We find a phase transition from graphene to graphdiyne at $\mathcal{F} = -7.0$ N m^{-1}. We also consider bilayer, trilayer, and four-layered graphene and find that the addition of extra layers results in a linear dependence of γ with $\mathcal{F}$.

I. INTRODUCTION

The remarkable properties of diamond are wide ranging and very well known.[1] Over the years a keen interest in diamond generated a very extensive search for diamond-related materials with similar properties to diamond and especially of its hardness. For instance, cubic boron nitride is a historically important material because of its diamondlike properties[2] and now it is produced on an industrial scale.

The bulk modulus for cubic boron nitride is in the range of 369 to 400 GPa,[3,4] whereas that for diamond is 442 GPa.[5] Other materials with good strength properties that are modeled on diamond (the bulk modulus in GPa is in brackets) include Si_3N_4 (290)[6] and C_3N_4 (496),[7] both in the spinel structures, and SiC (211),[5] AlN (212),[8] and GaN (202)[9] in the zinc-blend structures. Some of these structures are only accessible under conditions of high pressure, for example Si_3N_4.

With the recent discoveries of graphene,[10] a two-dimensional (2D) allotrope of carbon in the honeycomb structure and of boronitrene,[11] also in the honeycomb structure, one is once again alerted to the isostructural nature of these elements which prompts questions about the relative hardness and strength of these materials. The resistance to uniaxial strain (the 2D Young's modulus) of graphene and boronitrene has been compared theoretically[12] and experimentally measured,[13,14] showing that graphene is the stronger material in this respect. A 2D bulk modulus has been calculated for both materials based on empirically derived elastic constants,[15,16] and it is apparent that boronitrene has a value of approximately 85% of the value for graphene. The full significance of this result and how it describes the reaction of these materials to conditions of applied 2D pressure (which we refer to as force per unit length $\mathcal{F}$) has not been investigated. Also, since graphene and boronitrene are, in effect, among the first two-dimensional systems to be synthesized, the notion of hardness in two-dimensional systems is yet to be fully investigated and tested. For example, while three-dimensional crystal systems are compliant to positive isotropic pressure, it is generally considered not feasible to apply negative isotropic pressure in a carefully controlled manner to three-dimensional systems. Two-dimensional systems, on the other hand, open the prospects of applying a negative $\mathcal{F}$, which amounts to a uniform stretch of the material. In fact, it could be argued that stretching a two-dimensional material is mechanically more stable than uniformly compressing it in two dimensions. Stretching constrains the system in two dimensions, whereas compressing could result in buckling. Because of this latter point, it is essential that one views graphene and boronitrene as quasi-two-dimensional systems rather than truly two-dimensional systems. Also, puckering can occur for example by the inclusion of adatoms. Notwithstanding this, both stretching and compressing forces can, in principle, be applied in the plane of a two-dimensional material, and this opens a new terrain for investigating the mechanical properties of these materials. For instance, although the 2D bulk modulus is readily computed from the elastic constants, there exists no equation of state (EOS), as is the case for bulk materials, where this property can be deduced from the relationship of the hydrostatic change in surface area to $\mathcal{F}$. The possibility of 2D allotropes, as in the case of graphene,[17–20] also poses the question of whether phase transitions exist between these structures, something which can easily be tested by an EOS.

In this paper, we present an EOS applicable to 2D structures which provides a simple way to calculate the 2D bulk modulus. This modulus is a measure of the material's resilience to an externally applied isotropic $\mathcal{F}$ that is applied in two dimensions. It has units of force per unit length (N m^{-1}) and may be defined for a single layer as well as for multilayers. Because of this and the fact that a bulk modulus is associated with bulk

pressure, we refer to this 2D equivalent as the layer modulus (symbol γ). This property has many analogies in other fields of study such as the "membrane stretching modulus" (also known as the "area-stretching elastic constant") used in the study of lipid bilayer membranes[21] and other soft materials.

We use the EOS to extract fit parameters, including the layer modulus, for the monolayer systems of graphene (which we refer to as C) and boronitrene (also know as single-layer boron nitride, which we refer to as BN), and we also include results for Si, Ge, GeC, and SiC in the isostructural honeycomb structure for comparison. We consider four graphene allotropes to test the possibility of 2D phase transitions from graphene. We also consider bilayer, trilayer, and four-layered graphene (henceforth denoted as two-graphene, three-graphene, and four-graphene) to discover if the EOS can indicate any trends. In all cases, the elastic properties are calculated and the EOS is used to predict intrinsic strength.

In Sec. II, we present the theoretical concepts and equation of state used to investigate the two-dimensional systems as well as the computational parameters. In Sec. III we apply our methods to various 2D systems, and we present and discuss our findings. Lastly, in Sec. IV, we give our conclusions and suggest possible future work.

II. THEORETICAL FRAMEWORK

A. Two-dimensional equation of state

The two-dimensional equivalent of bulk pressure is force per unit length (denoted $\mathcal{F}$) where an in-plane hydrostatic force causes a uniform change in area of the two-dimensional lattice. Force per unit length is expressed as the first derivative of the energy with respect to surface area:

$$\mathcal{F} = -\frac{\partial E}{\partial A} \tag{1}$$

and has units N m^{-1}. Positive $\mathcal{F}$ represents a hydrostatic 2D compression while negative $\mathcal{F}$ represents a uniform stretching. The two-dimensional equivalent of the bulk modulus, which we refer to as the layer modulus, is then defined as

$$\gamma = -A\frac{\partial \mathcal{F}}{\partial A}. \tag{2}$$

The bulk modulus represents the resistance of a bulk material to compression, whereas the layer modulus represents the resistance of a 2D material to stretching.

In 1989, Hanfland *et al*. proposed a one-dimensional linear Murnaghan EOS[22] to experimentally study the effect of bulk pressure on graphite. The equation related the change in lattice parameter r to the pressure as follows:

$$r/r_0 = [(\beta_0'/\beta_0)\,P + 1]^{-\beta_0'}, \tag{3}$$

where r could either be the in-plane parameter a or the out-of-plane parameter c and where

$$\beta_0 = -\left(\frac{\partial P}{\partial \ln r}\right)_{P=0} \tag{4}$$

is the linear modulus with respect to bulk pressure and β_0' is its pressure derivative. The layer modulus for a monolayer of graphitic material can be estimated by the in-plane linear modulus using

$$\gamma_0 \simeq \frac{t\,\beta_0}{2}, \tag{5}$$

where t is the layer thickness.

Using the procedure described by Birch in Ref. 23, one can derive a similar two-dimensional EOS relating the applied $\mathcal{F}$ to the surface area for any 2D material:

$$\mathcal{F} = -2\,\gamma_0\left\{\epsilon + (1-\gamma_0')\,\epsilon^2 + \tfrac{2}{3}[(1-\gamma_0')(2-\gamma_0') + \gamma_0\,\gamma_0'']\,\epsilon^3\right\}, \tag{6}$$

where the equibiaxial Eulerian strain is given by

$$\epsilon = \frac{1}{2}\left[1 - \frac{A_0}{A}\right], \tag{7}$$

and A_0, γ_0, γ_0', and γ_0'' are the equilibrium values for the unit-cell area, layer modulus, the force per unit length derivative, and the second derivative of the layer modulus at $\mathcal{F} = 0$. Integrating Eq. (6) with respect to A, we obtain the energy EOS:

$$E(A) = E_0 + 4\,A_0\,\gamma_0\left\{\tfrac{1}{2}\,\epsilon^2 + \tfrac{1}{3}(5-\gamma_0')\,\epsilon^3 + \tfrac{1}{6}[(1-\gamma_0')\,(8-\gamma_0') + \gamma_0\,\gamma_0'' + 18]\,\epsilon^4\right\}, \tag{8}$$

which can be fitted to hydrostatic expansion and compression data to extract A_0, γ_0, γ_0', and γ_0''. The resulting γ versus $\mathcal{F}$ curve is then given by

$$\gamma(\mathcal{F}) = \gamma_0 + \gamma_0'\,\mathcal{F} + \tfrac{1}{2}\,\gamma_0''\,\mathcal{F}^2. \tag{9}$$

The fitted energy versus area curves of various candidate allotropes will give an indication of the presence of phase transitions between structures.

B. Elastic theory

The four nonzero 2D elastic constants for square, rectangular, or hexagonal lattices are c_{11}, c_{22}, c_{12}, and c_{66} (using the standard Voigt notation: 1-xx, 2-yy, 6-xy) where, due to symmetry, the square and hexagonal structures have $c_{11} = c_{22}$ and hexagonal structures have the additional relation that $c_{66} = \frac{1}{2}(c_{11} - c_{12})$. The units for the elastic constants are the same as $\mathcal{F}$.

In terms of these elastic constants, the layer modulus is

$$\gamma = \tfrac{1}{4}(c_{11} + c_{22} + 2\,c_{12}), \tag{10}$$

the 2D Young's moduli (in-plane stiffness) for strains in the Cartesian [10] and [01] directions are

$$Y^{2D}_{[10]} = \frac{c_{11}\,c_{22} - c_{12}^2}{c_{22}} \quad \text{and} \quad Y^{2D}_{[01]} = \frac{c_{11}\,c_{22} - c_{12}^2}{c_{11}}, \tag{11}$$

the corresponding Poisson's ratios are

$$\nu^{2D}_{[10]} = c_{12}/c_{22} \quad \text{and} \quad \nu^{2D}_{[01]} = c_{12}/c_{11}, \tag{12}$$

and the 2D shear modulus is

$$G^{2D} = c_{66}. \tag{13}$$

Since these equations apply only to the underlying 2D lattice of the material, they ignore the fact that the material has an out-of-plane thickness t. They can be reexpressed in the bulk units of N m^{-2} by dividing the desired modulus by the material thickness.

C. Computational details

All calculations were done within the framework of density-functional theory[24] using the projector augmented wave[25] formalism as implemented in VASP.[26] We used the Perdew-Burke-Ernzerhof (PBE) generalized gradient approximation (GGA) exchange-correlation functional[27] except for multilayer graphene where the local-density approximation (LDA) was used since it better incorporates the bonding between layers. The **k**-point sampling was done on a $10\times10\times1$ Monkhorst-Pack[28] grid for honeycomb and layered graphene structures. A grid of $4\times4\times1$ was used for structures with 4 or 8 atom unit cells and $2\times2\times1$ for 18 atom unit cells. The total-energy calculations were converged to within 10^{-5} eV and the Fermi distribution function with a smearing parameter of 0.2 eV was used to integrate the bands at the Fermi level. Each structure was relaxed so that the forces converged to within 0.01 eV Å^{-1}.

In all cases, a kinetic-energy cutoff of 500 eV was used. For the monolayer materials and two-graphene, the unit-cell height was set to $c = 15$ Å in order to prevent spurious interactions between unit cells repeating perpendicular to the layer plane. A height of 20 Å was used for three-graphene and a height of 30 Å was used for four-graphene to incorporate the extra layers while still preventing these interactions.

Elastic constants were obtained using the method of least-squares fit[29] as implemented in the MedeA-MT module. Phonon dispersions were obtained using the direct method as implemented in the MedeA-PHONON[30] module.

III. RESULTS AND DISCUSSION

A. Structures considered

In this study, we considered C, BN, SiC, GeC, Si, and Ge in the honeycomb structure as well as the four allotropes of graphene shown in Fig. 1. Multilayered graphene was also studied to investigate layer effects.

The relaxed honeycomb structures gave lattice constants calculated in GGA of 2.47, 2.51, 3.10, 3.24, 3.87, and 4.04 Å for C, BN, SiC, GeC, Si, and Ge, respectively. These values are in good agreement with the LDA results of 2.46, 2.51, 3.07, 3.22, 3.83, and 3.97 Å given by Ref. 12 with our values being slightly higher as is expected with GGA. Graphene, BN, GeC, and SiC are planar structures, whereas Si and Ge are buckled. Sahin *et al.*[12] calculated buckling parameters of $\Delta_{Si} = 0.44$ Å

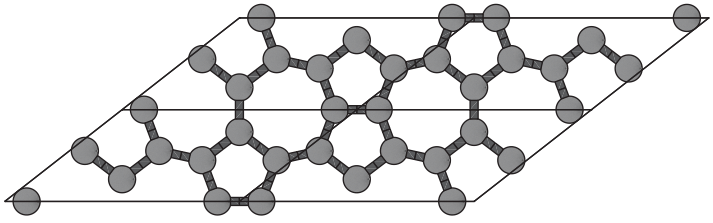

(a) 2x2 supercell

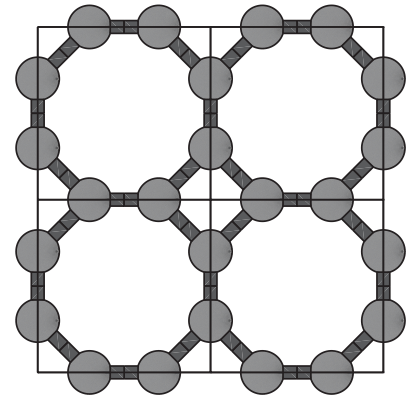

(b) 2x2 supercell

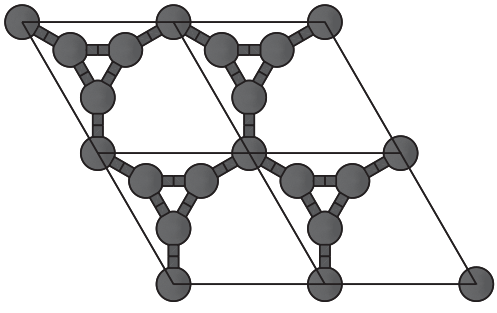

(c) 2x2 supercell

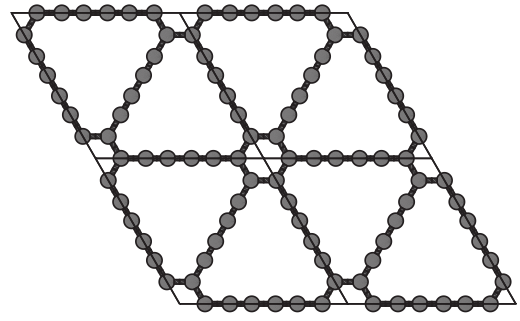

(d) 2x2 supercell

FIG. 1. The four graphene allotropes: (a) C1 (pentaheptite) consisting of pentagons and heptagons, (b) C2 consisting of squares and octagons, (c) C3 consisting of triangles and enneagons, and (d) C4 (graphdiyne) consisting of two acetylenic linkages between hexagons.

and $\Delta_{Ge} = 0.64$ Å for Si and Ge which are similar to our values of 0.45 and 0.68 Å , respectively.

Figure 1(a) shows the structure for C1 where the planar surface consists of distorted heptagons and pentagons with eight atoms per unit cell and *cmm* symmetry. This structure, called pentaheptite, has been previously studied using tight-binding methods which predict it to be metallic.[17,20] The relaxed optimized structure has unit-cell parameters of $a = 7.48$ Å and $b = 4.75$ Å with an internal angle of 38.05° which corresponds to a rectangular conventional cell of $a = 7.48$ Å and $b = 5.86$ Å. This compares well with the values of $a = 7.54$ Å and $b = 4.78$ Å obtained by Ref. 17 and the conventional cell values of $a = 7.56$ Å and $b = 5.70$ Å obtained by Ref. 20. Each pentagon is symmetrical about a midline that bisects an angle of 105.4°. The angles in circular order are 105.4, 106.9, 110.4, 110.4, and 106.9°, all which are distorted from the ideal value of 108°. Each heptagon is symmetrical about a midline bisecting an angle of 139.2° with angles in circular order of 139.2, 122.7, 130.4, 127.3, 127.3, 130.4, and 122.7°, all distorted from the ideal value of 128.6°. The average bond distance is $d_{C-C} = 1.43$ Å.

The graphene allotrope C2 shown in Fig. 1(b) is predicted to be a planar metallic[20] structure composed of squares connecting distorted octagons with four atoms per unit cell and *p*4*m* symmetry. The relaxed unit-cell lattice parameter of $a = 3.45$ Å compares well with the value of 3.47 Å obtained by Ref. 20. The internal angles for the octagons all have the same ideal value of 135° and the squares have $d_{C-C} = 1.46$ Å. The average bond distance is $d_{C-C} = 1.44$ Å.

The graphene allotrope C3, shown in Fig. 1(c), is obtained from the honeycomb structure by replacing the second atom in the unit cell by a group of three atoms in an equilateral triangular cluster giving four atoms per unit cell with *p*3*m*1 symmetry. The relaxed planar structure has a cell parameter of $a = 3.84$ Å with the triangle having $d_{C-C} = 1.40$ Å. The average bond length is $d_{C-C} = 1.41$ Å.

The C4 shown in Fig. 1(d) is known as graphdiyne[31] and consists of hexagons connected together by two acytylenic linkages in *p*6*m* symmetry forming a planar structure with an 18 atom unit cell. This allotrope is predicted to be metallic[20,32] and has recently been synthesized using a cross-coupling reaction.[33] The relaxed structure has a lattice parameter of $a = 9.47$ Å which compares well with the value of 9.44 Å obtained by Ref. 32 using a full-potential LDA linear combination of atomic orbitals method. Each hexagon has $d_{C-C} = 1.43$ Å while the acytylenic linkages have C-C bond lengths going between each hexagon of 1.40, 1.23, 1.34, 1.23, and 1.40 Å.

The monolayer and multilayered graphene structures used to study layer effects all had the same LDA calculated lattice parameter of $a = 2.45$ Å with the multilayered structures having a layer thickness of 3.33 Å in the conventional Bernal stacking arrangement.

B. Mechanical properties

Bulk equations of state such as the Birch equation are only valid for expansions and compressions in a range of ±10% about the equilibrium volume. The range of validity for our energy EOS was found by fitting energy versus unit-cell area

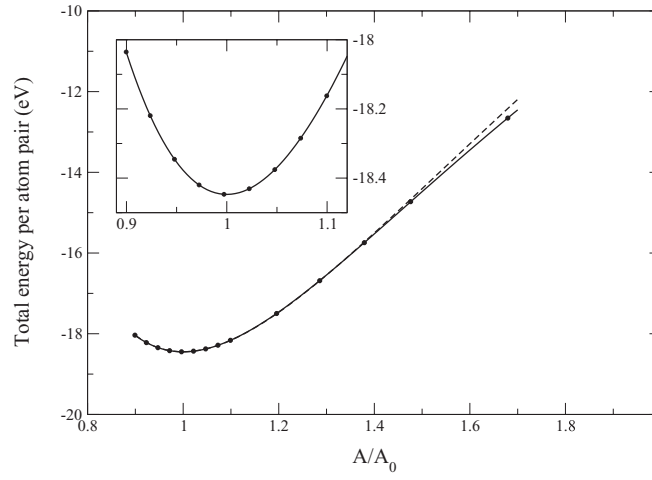

FIG. 2. EOS fit for graphene under hydrostatic strain showing total energy vs relative area A/A_0. Solid line shows the fit for all 14 calculated points in the range $0.9 < A/A_0 < 1.7$ (inset shows detail), and dashed line shows the fit for the first nine points in the range $0.9 < A/A_0 < 1.1$ extended to 1.7.

points for graphene. Calculations were done for 14 points in the range of 90 to 170% of the expected equilibrium area. One fit used nine points within 10% on either side of the expected equilibrium point while a second fit used the entire range. These are shown in Fig. 2 with the first fit shown as a dashed line and the second shown as a solid line. Although both fits overlap within the ±10% range, as shown by the inset plot for this range, it is clear that the narrower fit deviates from the calculated data points for predicted expansions beyond about 130–140% of the equilibrium area. The first fit gave EOS fit parameters of equilibrium lattice constant $a = 2.47$ Å, layer modulus $\gamma = 206.7$ N m^{-1}, force per unit length derivative $\gamma' = 4.33$, double force per unit length derivative $\gamma'' = -0.0306$ m N^{-1}, and a cohesive energy per atom pair of 15.2 eV while the second fit gave $a = 2.47$ Å, $\gamma = 207.1$ N m^{-1}, $\gamma' = 3.93$, $\gamma'' = -0.0670$ m N^{-1}, and the

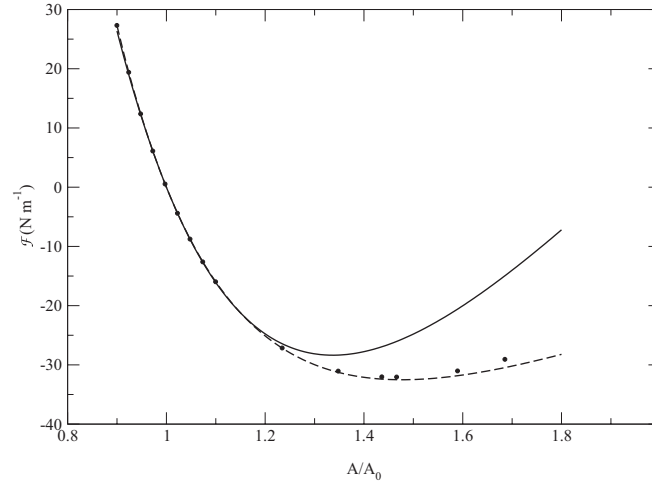

FIG. 3. Force per unit length vs relative area (A/A_0) for graphene showing a dashed line for the curve predicted by the $0.9 < A/A_0 < 1.1$ EOS fit and a solid line for the $0.9 < A/A_0 < 1.7$ prediction. Solid circles indicate calculated $\mathcal{F}$.

same cohesive energy. These fit parameters can be used in Eq. (6) to predict the $\mathcal{F}(A)$ curves for each fit. Figure 3 shows these curves for graphene using the two different sets of EOS fit parameters. The dashed line is the curve predicted by the first fit while the solid line is that for the larger fit. The solid data points are the force per unit length values calculated by VASP at each unit-cell area point. The figure shows that the two curves pass through the calculated $\mathcal{F}$ points up to $A/A_0 \sim 1.10$ but that the curve based on the larger fit deviates from the points beyond $A/A_0 \sim 1.15$. For this reason, it was decided to use the shorter range of $\pm 10\%$ to obtain EOS fit parameters for all materials.

The EOS fits in the upper section of Table I for the monolayer honeycomb structures are listed in order of decreasing layer modulus. They give lattice constant values that are identical to those obtained by structural relaxation. Our results show that graphene is the most resilient to stretching with a value of $\gamma_C = 206.6$ N m^{-1}. This is in agreement with the estimated average value of 209.4 N m^{-1} derived from the value of β_0 for graphite measured by Hanfland *et al*. with their linear Murnaghan EOS. Second is BN with $\gamma_{BN} = 177.0$ N m^{-1}, which is about ~85% of the value of graphene, which is the result reflected in the values by Michel and Verberck.[15,16] The results for SiC and GeC are $\gamma_{SiC} = 116.5$ N m^{-1} and $\gamma_{GeC} = 101.0$ N m^{-1}, being 56 and 49% that of graphene, respectively. The values for the buckled materials are $\gamma_{Si} = 44.5$ N m^{-1} and $\gamma_{Ge} = 29.6$ N m^{-1}, which are substantially lower than the results for graphene and boronitrene. This establishes the relative expandability of these isostructural materials, with Ge being the most expandable and graphene the least, and it verifies that graphene and boronitrene are ideal materials to use in applications that require structural integrity and a rigid membrane.

The results for the graphene allotropes are shown in the middle section of Table I and indicate that the layer modulus decreases from C→C1→C2→C3→C4 with values of $\gamma_{C1} = 192.3$ N m^{-1}, $\gamma_{C2} = 174.7$ N m^{-1}, $\gamma_{C3} = 153.2$ N m^{-1}, and $\gamma_{C4} = 110.2$ N m^{-1}. This establishes the relative expandability of these graphene allotropes, with C4 being the most expandable and graphene the least. The EOS fits shown in Fig. 5 show graphene as the most energetically stable 2D carbon allotrope with a phase transition existing from graphene to C4 at $\mathcal{F} = -7.0$ N m^{-1}.

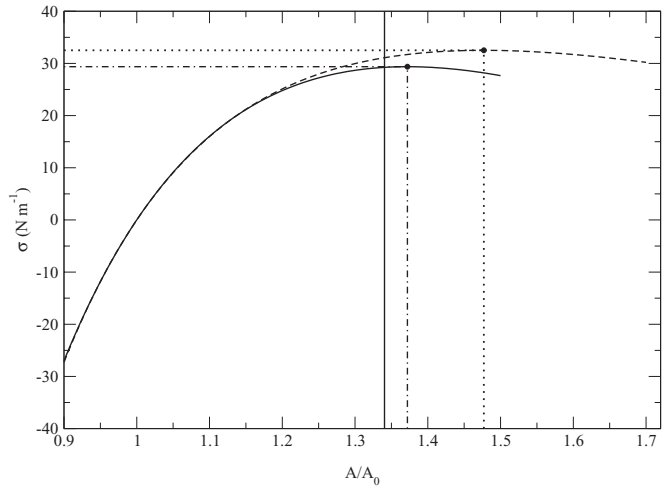

FIG. 4. Stress vs relative area (A/A_0) for graphene showing a dashed line for the $0.9 < A/A_0 < 1.1$ fit and a solid line for the $0.9 < A/A_0 < 1.477$ fit. Dotted and dash-dotted lines show predicted maximum values for each fit, while the solid vertical line is the value at which the phonon dispersion has an onset of a soft mode at K.

The force per unit length derivatives of γ for the planar structures have $4.33 \leqslant \gamma' \leqslant 5.33$ and $|\gamma''| < 0.075$ m N^{-1}. This means that according to Eq. (9) the layer moduli for these materials change in a similar near-linear manner in response

TABLE I. EOS fit parameters for honeycomb structures, graphene allotropes, and layered graphene (equilibrium area per atom pair A_0 in Å^2, lattice constants a and b, relaxed interlayer distance t and buckling parameter Δ in Å, layer modulus γ_0 in N m^{-1}, γ_0' dimensionless, γ_0'' in m N^{-1}, and cohesive energy per atom pair E_{coh} in eV).

	A_0	a	b	γ_0	γ_0'	γ_0''	E_{coh}
C	5.277	2.47		206.6	4.33	− 0.0306	15.2
BN	5.468	2.51		177.0	4.37	− 0.0454	13.8
SiC	8.303	3.10		116.5	4.79	− 0.0688	11.2
GeC	9.068	3.24		101.0	5.33	− 0.0722	9.3
Si	12.959	3.87[a]		44.5	1.79	− 0.6826	7.2
Ge	14.171	4.04[b]		29.6	4.23	− 1.5710	5.8
C1	5.480	7.48	4.75	192.3	4.35	− 0.0338	14.7
C2	5.944	3.45		174.7	4.33	− 0.0361	14.2
C3	6.399	3.84		153.2	4.55	− 0.0511	13.8
C4	8.629	9.47		110.2	4.51	− 0.0742	13.7
Four-graphene (LDA)	5.187	2.45[c]		863.4	4.29	− 0.0072	17.0
Three-graphene (LDA)	5.187	2.45[c]		647.6	4.29	− 0.0096	17.0
Two-graphene (LDA)	5.187	2.45[c]		431.8	4.28	− 0.0146	17.0
Graphene (LDA)	5.186	2.45		215.9	4.28	− 0.0286	17.0

[a] $\Delta = 0.45$.
[b] $\Delta = 0.68$.
[c] Atom relaxation for 2D EOS gave $t = 3.33$.

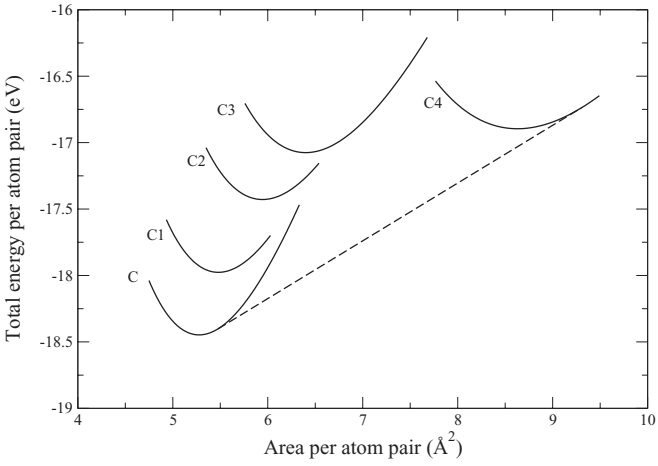

FIG. 5. EOS for graphene and four allotropes showing a phase transition from graphene to C4 at $\mathcal{F} = -7.0$ N m^{-1}.

to small changes in $\mathcal{F}$ around their equilibrium structures. The buckled structures of Ge and Si react in a more parabolic manner with the layer modulus for Ge having more curvature than Si, since $|\gamma''_{\mathrm{Si}}| < |\gamma''_{\mathrm{Ge}}|$. This could be the result of the greater buckling in the structure for Ge.

The lower section of Table I shows the LDA EOS fits for one-, two-, three-, and four-layered graphene. The layer modulus for two-graphene is exactly twice that of monolayer graphene with a value of 431.8 N m^{-1}, while three-graphene and four-graphene have values exactly three times and four times as much, respectively. This establishes γ as a true property of layered structures with its value scaling with the number of atomic layers n as $\gamma = 215.9\,n$. The material becomes more resilient to stretching with the addition of extra layers as would be expected. All have values for γ' are around 4.28, indicating that to first order the layer moduli for these layered structures all change by the same amount for the same change in $\mathcal{F}$. The values for γ'' are inversely proportional to the number of layers scaling as $\gamma'' = -0.0286/n$. This indicates that $\gamma(\mathcal{F})$ becomes increasingly linear around the equilibrium value with an increase in the number of layers.

The calculated cohesive energies per atom pair show a general decreasing trend going down the column, with C having the largest value and Si the lowest. Our values for honeycomb C, BN, SiC, GeC, Si, and Ge are lower than the values of 20.08, 17.65, 15.25, 13.23, 10.32, and 8.30 eV given by Ref. 12 due to the underbinding nature of GGA. The C allotropes have similar cohesive energies, as do the layered graphenes.

C. Elastic properties

The two-dimensional elastic constants c_{ij} were obtained by first doing a least-squares fit on various *ab initio* stress calculations for carefully chosen strain states on the volume unit cell to extract the bulk elastic constants.[29] These were then multiplied by the unit-cell height to obtain the corresponding 2D values. Due to the size of the unit-cell heights, all bulk elastic constants containing 4 or 5 in their subscripts equated to zero within the numerical error of the fit. Monolayer materials also had all elastic constants containing 3 in their subscripts calculated to zero. The elastic constants for the various structures and other derived elastic properties are listed in Table II.

TABLE II. Elastic properties for honeycomb structures, graphene allotropes, and layered graphene (elastic constants c_{ij}, shear modulus G^{2D}, calculated layer modulus γ_{calc}, EOS-derived layer modulus given in brackets, Young's modulus Y^{2D} in N m^{-1}, and Poisson's ratio ν dimensionless).

		c_{11}	c_{22}	c_{12}	$c_{66} = G^{2D}$	γ_{calc}	$Y^{2D}_{[10]}$	$Y^{2D}_{[01]}$	$\nu_{[10]}$	$\nu_{[01]}$
C	This work	352.7	352.7	60.9	145.9	206.8 (206.6)	342.2	342.2	0.173	0.173
	VASP (PBE)[34]	358.1	358.1	60.4	148.9[a]	209.3[a]	348	348	0.169	0.169
	Estimated[35]	372.2	372.2	46.6	162.8	209.4	366.4	366.4	0.125	0.125
BN	This work	289.8	289.8	63.7	113.1	176.8 (177.0)	275.8	275.8	0.220	0.220
	Estimated[36]	270.0	270.0	56.2	106.9	163.1	258.3	258.3	0.208	0.208
SiC	This work	179.7	179.7	53.9	62.9	116.8 (116.5)	163.5	163.5	0.300	0.300
GeC	This work	154.7	154.7	47.5	53.6	101.1 (101.0)	140.1	140.1	0.307	0.307
Si	This work	68.3	68.3	23.3	22.5	45.8 (44.5)	60.6	60.6	0.341	0.341
	VASP (LDA)[37]	68.9	68.9	23.3	22.8[a]	46.1[a]	61.0	61.0	0.33	0.33
Ge	This work	46.4	46.4	13.1	16.7	29.8 (29.6)	42.7	42.7	0.282	0.282
	VASP (LDA)[37]	47.3	47.3	16.7	15.3[a]	32.0[a]	41.4	41.4	0.35	0.35
C1	This work	309.6	325.2	67.6	117.8	192.5 (192.3)	295.5	310.4	0.208	0.218
C2	This work	295.3	295.3	54.5	49.1	174.9 (174.7)	285.2	285.2	0.185	0.185
C3	This work	219.4	219.4	87.7	65.9	153.6 (153.2)	184.3	184.3	0.400	0.400
C4	This work	152.1	152.1	69.0	41.6	110.6 (110.2)	120.8	120.8	0.454	0.454
Four-graphene (LDA)	This work	1456.2	1456.2	273.8	591.2	865.0 (863.4)	1404.7	1404.7	0.188	0.188
Three-graphene (LDA)	This work	1091.9	1091.9	204.7	443.9	648.3 (647.6)	1053.5	1053.5	0.187	0.187
Two-graphene (LDA)	This work	728.5	728.5	135.9	296.3	432.2 (431.8)	703.1	703.1	0.186	0.186
Graphene (LDA)	This work	364.6	364.6	67.3	148.7	216.0 (215.9)	352.2	352.2	0.185	0.185

[a]Calculated from given elastic constants.

In order to validate our method, we compared our results for C, BN, Si, and Ge to previous calculations and results based on available experimental data. The results for graphene compare very well with those of Ref. 34, which used a least-squares fit of Cauchy stress calculations done in VASP using the PBE GGA functional. As with our method, Ref. 34 converted bulk volume unit-cell values to planar values by multiplying by the cell height. As can be seen in Table II, the values in Ref. 34 for the elastic constants, the moduli, and the Poisson ratio are very close to our results. Our values also compare reasonably well with those derived from elastic constant estimates taken from inelastic x-ray data for graphite,[35] and our value of 342.2 N m^{-1} for the 2D Young's modulus compares well to the experimental value of 340 ± 50 N m^{-1} measured by Lee *et al.*[13] The results for BN compare reasonably well with those derived from elastic constant estimates from inelastic x-ray data for hexagonal boron nitride.[36] Our value of 275.8 N m^{-1} for the 2D Young's modulus is within the range of 200–500 N m^{-1} determined by Song *et al.*[14] For the two nonplanar materials Si and Ge, the values for the elastic constants, moduli, and Poisson's ratio compare very well with those calculated by Ref. 37, which used various strain-energy LDA calculations to obtain their elastic constants.

What is immediately apparent about the values in Table II is that the γ_{calc} values derived from the elastic constants are almost exactly the same as the layer modulus values obtained from the EOS fits (shown in brackets). This independently establishes that our EOS correctly determines the layer modulus for planar 2D materials as well as buckled and layered quasi-two-dimensional systems.

The elastic properties for the six honeycomb systems are shown in the top section of Table II. All the moduli show a decreasing trend going down the columns from C→BN→SiC→GeC→Ge→Si. The Young's moduli values of 342.2, 275.8, 163.5, 140.1, 60.6, and 42.7 N m^{-1} are in general agreement with the LDA values of 335, 267, 166, 142, 62, and 48 N m^{-1} given by Ref. 12. The Poisson's ratios show an increasing trend except where Ge and Si are switched due to Ge being more buckled. Since these structures are isostructural, these trends are indicative of the relative bonding strengths between the atoms, and not of the geometry of the materials, except in the case of Si and Ge where the added effect of surface buckling further reduces their elastic moduli.

The elastic properties of the graphene allotropes are shown in the middle section. There is a clear decrease in Young's modulus going down the columns, with C1 having the highest anisotropic values of $Y^{2D}_{[10]} = 295.5$ N m^{-1} and $Y^{2D}_{[01]} = 310.4$ N m^{-1}. Due to the fact that the pentagons are symmetrical about their y axis and the enneagons are symmetrical about their x axis, C1 is slightly more structurally rigid to elongations along the [01] direction. The averaged Young's modulus of 303.0 N m^{-1} is 88% that of graphene. Next is C2 with an isotropic value of 83% that of graphene. C1 and C2 have comparable Young's moduli with C2 having a value 94% that of the averaged value for C1, indicating that they have a similar resilience to linear strain. C3 has a value 54% that of graphene and 65% that of C2. This is due to increased bond bending as compared to the previous structures. C4 has the lowest value, being 35% that of graphene and 66% that of C3. The long acetylenic linkages cause structural weakness compared with the more compact structures. Graphene has the highest shear modulus due to the fact that its honeycomb structure is very rigid. The shear modulus of C1 is ~81% that of graphene due to its strong network of slightly distorted polygons. The shear moduli of C2 and C3 are more than half that of graphene, showing them to be more prone to bond bending under shear strain. Even through C4 has a generalized honeycomb structure similar to graphene, it has a shear modulus ~30% that of graphene due to the long acetylenic chains making up this structure. The Poisson's ratios for C3 and C4 are significantly higher than C1 and C2 due to their structures lending more to bond bending under uniaxial strain. These results show that of all the allotropes metallic C1 would best compliment graphene for nanoapplications since both have comparable moduli and therefore similar hardness properties.

The last section of Table II shows the results for the layered graphene structures. The elastic constants c_{11}, c_{22}, c_{12}, and c_{66} (and therefore all derived elastic moduli) scale in the same manner as found for γ. This is seen in the experimental results of Song *et al.*,[14] who gave Young's modulus values of $503 \pm 30, 431 \pm 21$, and 223 ± 16 N m^{-1} for BN samples with possible layer numbers of 5, 4, and 2. The moduli reflect this scaling by having possible ratios of 5/4, 5/2, and 2 within the experimental error. The Poisson ratios for the layered materials are in the range $0.185 \leqslant \nu \leqslant 0.188$, showing that the widths of the materials all decrease the same with the same amount of linear strain.

In general, the Young's and shear moduli rank in the same order as the layer modulus, showing that it is a good indication of relative hardness.

D. Intrinsic strength

When a 2D material is stretched, the applied stress increases with the strain until it reaches a maximum beyond which the stress decreases. This extremum point indicates the isotropic intrinsic stress and strain for the material at which point the material fails. These values can be obtained by using Eq. (6) with the fit parameters from the 2D EOS fit for a given material. Figure 4 shows the stress (negative $\mathcal{F}$) versus relative area (A/A_0) curves for graphene using two different EOS fits. The dashed curve is from a fit over the range $0.9 < A/A_0 < 1.1$ and predicts a breaking stress of 32.5 N m^{-1} at an area 47.7% larger than the equilibrium value. The actual onset of a soft mode in the phonon dispersion occurs when $A/A_0 = 1.340$ (the solid vertical line in Fig. 4), showing that this curve overestimates A/A_0 by 10.2%. The solid curve in Fig. 4 uses an EOS fit that has the previously predicted relative area of 1.477 as an upper bound. It predicts a slightly lower failure stress of 29.4 N m^{-1} at a relative area of 1.372. This predicted area is closer to the phonon prediction, being only 2.4% higher.

The predicted results for our materials using this method are summarized in Table III. The materials in the upper section are listed in order of decreasing layer modulus. The relative area and breaking stress x_A and σ_A are based on a ±10% EOS fit while x_B and σ_B use the extended range. The predicted phonon results for selected examples of planar, buckled, and layered

TABLE III. Intrinsic strength based on EOS fits for honeycomb structures, graphene allotropes, and layered graphene (x_A is the relative area at failure from the EOS fit over $0.9 < A/A_0 < 1.1$, σ_A is the hydrostatic stress at failure from the same fit in N m^{-1}, x_B is the relative area at failure from the EOS fit over $0.9 < A/A_0 < x_A$, σ_B is the hydrostatic stress at failure from the same fit in N m^{-1}, x_{phonon} is the relative area where the first onset of a soft mode occurs in the phonon dispersion, and RD is the relative percentage difference between x_B and x_{phonon}).

	x_A	σ_A	x_B	σ_B	x_{phonon}	RD (%)[a]
C	1.477	32.5	1.372	29.4	1.340	2.4
BN	1.487	28.0	1.407	26.0	1.365	3.1
SiC	1.414	16.4	1.253	13.3	1.427	− 12.2
GeC	1.449	13.9	1.244	10.5	1.386	− 10.2
Si	1.301	6.6	1.201	4.9	1.420	− 15.4
Ge	1.200	2.9	1.239	3.2	1.430	− 12.7
C1	1.469	30.0	1.278	24.3	1.309	− 2.4
C2	1.464	27.5	1.298	22.7	1.309	− 0.8
C3	1.422	22.3	1.304	19.4	1.308	− 0.3
C4	1.414	16.0	1.307	14.0		
Four-graphene (LDA)	1.481	137.0	1.381	125.0		
Three-graphene (LDA)	1.481	102.8	1.381	93.8	1.32	4.6
Two-graphene (LDA)	1.478	68.4	1.381	62.5	1.363	1.3
Graphene (LDA)	1.483	34.4	1.383	31.3	1.363	1.5

[a]Relative difference, $\frac{x_B - x_{\text{phonon}}}{x_{\text{phonon}}} \times 100\%$.

materials are compared to the EOS predictions by calculating the relative percentage difference between the two.

The results in the upper two sections of Table III show that C, BN, C1, C2, and C3 give predictions no greater than ∼3% off the phonon results while the results for SiC, GeC, Si, and Ge are more than 10% off. Of the elemental honeycomb structures C, Si, and Ge, only the buckled structures show a vast discrepancy between the EOS predictions and phonon results. Of the binary structures, only SiC and GeC have vast discrepancies between EOS and phonon predictions. Whereas BN contains atoms of comparable mass, SiC and GeC contain atoms with large mass differences. The layered materials of two-graphene and three-graphene show predicted EOS values no more than 5% off the phonon values. We suggest that the discrepancies are due to anharmonic effects that are not accounted for by the phonon calculations when the structures are extended too far from their equilibrium states.

The honeycomb structures in the upper section of Table III show decreasing intrinsic stress σ_B in the same ranking order as their layer moduli, with graphene having the highest value of 29.4 N m^{-1}. Boronitrene is second with a comparable breaking stress of 26.0 N m^{-1}. The values for SiC and GeC are 45 and 36% that of C. Si and Ge have the lowest values of 17 and 11% that of graphene.

The ordering of the intrinsic relative area x_B goes in decreasing order from BN→C→SiC→GeC→Ge→Si. BN and graphene both fail at areas ∼40% greater than their equilibrium values though at different stresses. SiC, GeC, and Ge fail at areas 24–25% greater while Si fails at a relative area 20% higher than its equilibrium value, about half that of BN and C. Ge has a higher intrinsic strain than Si even though it fails at a lower stress since it is more buckled. These results indicate that C and BN are able to withstand greater isotropic strains than the other honeycomb materials at higher stresses, a result reflected by their relatively high layer modulus values.

The intrinsic stress values of the four graphene allotropes, shown in the middle section of Table III, decrease from C1→C2→C3→C4, with C1 having a value 83% that of graphene, C2 (77%), C3 (66%), and C4 (48%). This correlates well with the ordering of their layer moduli. All of the structures fail at approximately the same strain with an area ∼30% higher than their equilibrium values. This is slightly lower than graphene, once again showing the honeycomb structure to be the strongest.

As with the elastic moduli, the intrinsic stress values of the layered graphene structures, shown in the lower section of Table III, scale with the number of layers. The values scale on average as $\sigma = 31.2\,n$ where n is the number of layers present while the relative area at failure remains fixed at ∼1.38, indicating that these structures all fail at the same lattice parameter of $a = 2.88$ Å. This shows that each added layer increases the strength of the multilayered structure but does not increase the amount of stretching the structure can withstand.

IV. CONCLUSIONS

In this paper we proposed an equation of state (EOS) for 2D materials that equates 2D pressure (force per unit length $\mathcal{F}$) with a change in surface area. This was then used to fit energy versus area data to extract equilibrium fit parameters including the layer modulus (symbol γ), which measures a material's resilience to hydrostatic stretching. We give results for the monolayer systems of graphene and boronitrene, and we also include results for Si, Ge, GeC, and SiC in the isostructural honeycomb structure for comparison. For these structures, the layer moduli were ranked, showing graphene to be the most resilient to stretching with $\gamma_{\text{C}} = 206.6$ N m^{-1} followed by boronitrene with a value of $\gamma_{\text{BN}} = 177.0$ N m^{-1}. The buckled structures of Si and Ge were found to be the least resilient. It was found that $\gamma(\mathcal{F})$ around $\mathcal{F} = 0$ is more

linear for planar structures and more parabolic for buckled structures. We considered four graphene allotropes including pentaheptite and graphdiyne. For the graphene allotropes, the ranking for γ in decreasing order went C1→C2→C3→C4 with C1 (pentaheptite) having a value comparable to graphene. C4 (graphdiyne) was shown to be the softest of the four. The EOS fits for these structures showed a phase transition from graphene to C4 at a force per unit length of -7 N m^{-1}. We considered multilayered graphene, and it was found that the curve $\gamma(\mathcal{F})$ is more linear around $\mathcal{F}=0$ as the number of layers is increased. The planar elastic constants for all the structures were calculated, and it was found that the layer modulus derived from the elastic constants matched those from the EOS fits, thereby independently verifying the EOS. It was also found that, in general, the other moduli rank according to the layer modulus. The EOS was used to predict the isotropic intrinsic strength of the various structures. The results show that the intrinsic stress correlated well with the layer modulus, with graphene having the highest intrinsic strength of 29.4 N m^{-1} closely followed by boronitrene with 26.0 N m^{-1}.

Based on these results, we conclude that the layer modulus is a good indicator of relative hardness in planar, buckled, and layered 2D structures and that our proposed EOS correctly extracts this value as one of its fit parameters. We also conclude that the EOS is a useful tool to investigate a materials response to $\mathcal{F}$ and can be used to look for possible phase transitions.

Future work includes using the EOS to test how the adsorption of H atoms on graphene and bilayer graphene effects their strength and response to in-plane stretching.

ACKNOWLEDGMENTS

We are grateful to Jannie Pretorius for assistance with the implementation and the maintenance of the VASP codes. We also thank Kingsley Obodo for useful discussions and Prof. Richard Martin for the suggestion of the term "layer modulus" for γ. We are grateful to the University of Pretoria, the National Research Foundation and the National Institute for Theoretical Physics for financial support.

*richard.andrew@up.ac.za

[1] M. Willander, M. Friesel, Qamar-ul Wahab, and B. Straumal, J. Mater. Sci.: Mater. Electron. **17**, 1 (2006).
[2] R. H. Wentorf, J. Chem. Phys. **26**, 956 (1957).
[3] E. Knittle, R. M. Wentzcovitch, R. Jeanloz, and M. L. Cohen, Nature (London) **337**, 349 (1989).
[4] M. Grimsditch, E. S. Zouboulis, and A. Polian, J. Appl. Phys. **76**, 832 (1994).
[5] M. L. Cohen, Phys. Rev. B **32**, 7988 (1985).
[6] A. Zerr, M. Kempf, M. Schwarz, E. Kroke, M. Goken, and R. Riedel, J. Am. Ceram. Soc. **85**, 86 (2002).
[7] T. Wang, D. Yu, Y. Tian, F. Xiao, J. He, D. Li, W. Wang, and L. Li, Chem. Phys. Lett. **334**, 7 (2001).
[8] M. B. Kanoun, S. Goumri-Said, A. E. Merad, G. Merad, J. Cibert, and H. Aourag, Semicond. Sci. Technol. **19**, 1220 (2004).
[9] T. Tsuchiya, K. Kawamura, O. Ohtaka, H. Fukui, and T. Kikegawa, Solid State Commun. **121**, 555 (2002).
[10] K. S. Novoselov, A. K. Geim, S. V. Morozov, D. Jiang, Y. Zhang, S. V. Dubonos, I. V. Grigorieva, and A. A. Firsov, Science **306**, 666 (2004).
[11] K. S. Novoselov, D. Jiang, F. Schedin, T. J. Booth, V. V. Khotkevich, S. V. Morozov, and A. K. Geim, Proc. Natl. Acad. Sci. **102**, 10451 (2005).
[12] H. Şahin, S. Cahangirov, M. Topsakal, E. Bekaroglu, E. Akturk, R. T. Senger, and S. Ciraci, Phys. Rev. B **80**, 155453 (2009).
[13] C. Lee, X. Wei, J. W. Kysar, and J. Hone, Science **321**, 385 (2008).
[14] L. Song, L. Ci, H. Lu, P. B. Sorokin, C. Jin, J. Ni, A. G. Kvashnin, D. G. Kvashnin, J. Lou, B. I. Yakobson, and P. M. Ajayan, Nano Lett. **10**, 3209 (2010).
[15] K. H. Michel and B. Verberck, Phys. Rev. B **78**, 085424 (2008).
[16] K. H. Michel and B. Verberck, Phys. Rev. B **80**, 224301 (2009).
[17] V. H. Crespi, L. X. Benedict, M. L. Cohen, and S. G. Louie, Phys. Rev. B **53**, R13303 (1996).
[18] H. Terrones, M. Terrones, E. Hernández, N. Grobert, J.-C. Charlier, and P. M. Ajayan, Phys. Rev. Lett. **84**, 1716 (2000).
[19] M. Deza, P. W. Fowler, M. Shtogrin, and K. Vietze, J. Chem. Inf. Comput. Sci. **40**, 1325 (2000).
[20] A. N. Enyashin and A. L. Ivanovskii, Phys. Status Solidi B **248**, 1879 (2011).
[21] S. Kakorin, T. Liese, and E. Neumann, J. Phys. Chem. B **107**, 10243 (2003).
[22] M. Hanfland, H. Beister, and K. Syassen, Phys. Rev. B **39**, 12598 (1989).
[23] F. Birch, Phys. Rev. **71**, 809 (1947).
[24] P. Hohenberg and W. Kohn, Phys. Rev. **136**, 864 (1964).
[25] P. E. Blöchl, Phys. Rev. B **50**, 17953 (1994).
[26] G. Kresse and J. Furthmüller, Phys. Rev. B **54**, 11169 (1996).
[27] J. P. Perdew, K. Burke, and M. Ernzerhof, Phys. Rev. Lett. **77**, 3865 (1996).
[28] H. J. Monkhorst and J. D. Pack, Phys. Rev. B **13**, 5188 (1976).
[29] Y. Le Page and P. Saxe, Phys. Rev. B **65**, 104104 (2002).
[30] K. Parlinski, Z-.Q. Li, and Y. Kawazoe, Phys. Rev. Lett. **78**, 4063 (1997).
[31] M. M. Haley, S. C. Brand, and J. J. Pak, Angew. Chem. Int. Ed. Engl. **36**, 835 (1997).
[32] N. Narita, S. Nagai, S. Suzuki, and K. Nakao, Phys. Rev. B **58**, 11009 (1998).
[33] G. Li, Y. Li, H. Liu, Y. Guo, Y. Li, and D. Zhu, Chem. Commun. (Cambridge, England) **46**, 3256 (2010).
[34] X. Wei, B. Fragneaud, C. A. Marianetti, and J. W. Kysar, Phys. Rev. B **80**, 205407 (2009).
[35] A. Bosak, M. Krisch, M. Mohr, J. Maultzsch, and C. Thomsen, Phys. Rev. B **75**, 153408 (2007).
[36] A. Bosak, J. Serrano, M. Krisch, K. Watanabe, T. Taniguchi, and H. Kanda, Phys. Rev. B **73**, 041402 (2006).
[37] H. Zhang and R. Wang, Physica B: Condensed Matter **406**, 4080 (2011).